The Plant Cell, Vol. 25: 1368–1382, April 2013, www.plantcell.org © 2013 American Society of Plant Biologists. All rights reserved.

Arabidopsis Sec1/Munc18 Protein SEC11 Is a Competitive and Dynamic Modulator of SNARE Binding and SYP121-Dependent Vesicle Traffic[W][OA]

Rucha Karnik,[a] Christopher Grefen,[a] Robert Bayne,[a] Annegret Honsbein,[a] Tim Köhler,[b] Dimitrios Kioumourtzoglou,[c] Mary Williams,[d] Nia J. Bryant,[c] and Michael R. Blatt[a,1]

[a] Laboratory of Plant Physiology and Biophysics, University of Glasgow, Glasgow G12 8QQ, United Kingdom
[b] Botanical Institute, University of Darmstadt, D-64287 Darmstadt, Germany
[d] American Society of Plant Biologists, Rockville, Maryland 20855
[c] Cell Biology Laboratory, Institute of Molecular, Cell, and Systems Biology, University of Glasgow, Glasgow G12 8QQ, United Kingdom

The *Arabidopsis thaliana* Qa-SNARE SYP121 (=SYR1/PEN1) drives vesicle traffic at the plasma membrane of cells throughout the vegetative plant. It facilitates responses to drought, to the water stress hormone abscisic acid, and to pathogen attack, and it is essential for recovery from so-called programmed stomatal closure. How SYP121-mediated traffic is regulated is largely unknown, although it is thought to depend on formation of a fusion-competent SNARE core complex with the cognate partners VAMP721 and SNAP33. Like SYP121, the *Arabidopsis* Sec1/Munc18 protein SEC11 (=KEULE) is expressed throughout the vegetative plant. We find that SEC11 binds directly with SYP121 both in vitro and in vivo to affect secretory traffic. Binding occurs through two distinct modes, one requiring only SEC11 and SYP121 and the second dependent on assembly of a complex with VAMP721 and SNAP33. SEC11 competes dynamically for SYP121 binding with SNAP33 and VAMP721, and this competition is predicated by SEC11 association with the N terminus of SYP121. These and additional data are consistent with a model in which SYP121-mediated vesicle fusion is regulated by an unusual "handshaking" mechanism of concerted SEC11 debinding and rebinding. They also implicate one or more factors that alter or disrupt SEC11 association with the SYP121 N terminus as an early step initiating SNARE complex formation.

INTRODUCTION

Soluble *N*-ethylmaleimide–sensitive factor adaptor protein receptors (SNAREs) comprise a superfamily of proteins that mediate vesicle traffic by driving the fusion of vesicle and target membranes. Vesicle traffic in plants, as in other eukaryotes, is required for transport of membrane components, proteins, and soluble cargo between endomembrane compartments and across the plasma membrane to the apoplast (Pratelli et al., 2004; Jahn and Scheller, 2006; Bassham and Blatt, 2008). SNARE proteins localize to vesicle and target membranes where they bind their cognate SNARE partners to form a stable heteromeric core complex. Assembly of the core complex draws vesicle and target membranes together, overcoming the hydration energy of the membrane surfaces to allow fusion of the two bilayers. Cognate SNAREs in the complex contribute highly conserved Qa-, Qb-, Qc-, and R-SNARE motifs that are classified according to their structure and the amino acid (Gln or Arg) present at the center of the motif (Fasshauer et al., 1998; Bock et al., 2001). Qa-SNAREs, often referred to as syntaxins, are usually resident on the target membrane along with SNAP25-related (for synaptosome-associated protein of 25 kD) proteins, which contribute Qb- and Qc-motifs. Vesicle-associated membrane proteins (VAMPs) contribute the R-motif and are normally resident on the vesicle membrane.

The SNAREs of plants display the widest spatio-temporal distribution of all eukaryotes (Sanderfoot et al., 2000; Pratelli et al., 2004), an observation that has been interpreted to reflect the need for specialized functions in plant growth and homeostasis (Bassham and Blatt, 2008; Grefen and Blatt, 2008). Among these, the Qa-SNARE SYP121 (Syntaxin of Plants 121, =SYR1/PEN1) is of special interest because it is central to a repertoire of processes in plant growth and development as well as in physiological responses to biotic and abiotic stress. Not only is SYP121 important for general vesicle transport and secretion (Geelen et al., 2002; Sutter et al., 2006b; Tyrrell et al., 2007), but it also plays roles in cellular responses to drought and the water stress hormone abscisic acid (Leyman et al., 1999; Sutter et al., 2007; Eisenach et al., 2012), it facilitates targeted vesicle traffic for defense against pathogen attack (Collins et al., 2003; Kwon et al., 2008), and it interacts directly with K^+ channels to facilitate solute uptake for cell expansion and plant growth (Honsbein et al., 2009; Grefen et al., 2010a; Honsbein et al., 2011). The architecture of SYP121 is similar to that of other Qa-SNAREs (Blatt et al., 1999; Pratelli et al., 2004; Jahn and Scheller, 2006; Lipka et al., 2007). It incorporates a C-terminal

[1] Address correspondence to michael.blatt@glasgow.ac.uk.
The author responsible for distribution of materials integral to the findings presented in this article in accordance with the policy described in the Instructions for Authors (www.plantcell.org) is: Michael R. Blatt (michael.blatt@glasgow.ac.uk).
[W] Online version contains Web-only data.
[OA] Open Access articles can be viewed online without a subscription.
www.plantcell.org/cgi/doi/10.1105/tpc.112.108506

membrane anchor and an adjacent helical domain (H3) that harbors the Qa-SNARE motif, and it includes a set of three α-helices, the Habc domain, with an unstructured, N-terminal sequence of amino acids. The Habc domain is thought to fold back on the H3 helix in a so-called closed or inactive conformation, regulating access to the Qa-SNARE domain for binding with other SNAREs (Jahn and Scheller, 2006; Bassham and Blatt, 2008; Südhof and Rothman, 2009). SYP121 is known to interact with its cognate SNARE partners, SNAP33 and both VAMP721 and VAMP722, in a ternary SNARE core complex (Kwon et al., 2008). However, very little is known about how SYP121 function is controlled and how this control is achieved.

Mammalian SNAREs will interact promiscuously to form homo- and heteromeric complexes in solution (Weber et al., 1998; Jahn and Scheller, 2006). Therefore, it is generally recognized that additional factors control SNARE assembly to ensure the specificity of vesicle fusion in vivo. Among these, members of the Sec1/Munc18 (SM) family of proteins are known to interact with Qa-SNAREs (Dulubova et al., 1999, 2002, 2007; Hu et al., 2002). Their binding and associations with additional regulatory proteins, such as Munc13 (Rizo et al., 2012; Hughson, 2013; Ma et al., 2013), are thought to ensure the specificity of membrane fusion and to enhance the kinetics of the process (Shen et al., 2007). SM proteins interact with Qa-SNAREs through at least three binding modes, each with different consequences for formation of the SNARE complex (Burgoyne and Morgan, 2007; Südhof and Rothman, 2009), either stabilizing the Qa-SNARE in a closed conformation with the Habc α-helices, facilitating entry into SNARE core complex assembly, or stabilizing the Qa-SNARE in the core complex with its cognate SNARE partners.

Six SM proteins are known in *Arabidopsis thaliana* (Sanderfoot et al., 2000; Blatt and Thiel, 2003; Sutter et al., 2006a), two of which have been functionally associated with one or more Qa-SNAREs. The SM protein VPS45 positively regulates vesicular traffic with the SNAREs SYP41, SYP61, and VTI12 between the *trans*-Golgi network, early endosomes, and vacuole (Bassham et al., 2000; Zouhar et al., 2009), and SEC11 (=KEULE) binds the Qa-SNARE SYP111 (=KNOLLE) during cytokinesis (Waizenegger et al., 2000; Assaad et al., 2001). Of the other four SM proteins in *Arabidopsis*, SEC12 (=SEC1a) and SEC13 (=SEC1b) are expressed at very low levels or not at all (Sanderfoot et al., 2000; Bassham and Blatt, 2008); VPS33 associates with traffic at the vacuole (Rojo et al., 2003); and the remaining structural protein shows closest homology to the yeast SM proteins Sly1p, suggesting its association with endomembrane traffic between the endoplasmic reticulum and the Golgi (Blatt and Thiel, 2003). Therefore, it was of interest to us that SEC11 has been reported to play a role in root hair development independent of SYP111 (Assaad et al., 2001). SYP111 is expressed only during cell division and is localized to the cell plate; however, SEC11, like SYP121, is expressed constitutively throughout the vegetative plant, suggesting additional functions for this SM protein distinct from its role in cytokinesis. Furthermore, SEC11 is reported to occur in both soluble and plasma membrane–associated fractions (Halachmi and Lev, 1996; Assaad et al., 2001), as would be expected if SEC11 interacted with a plasma membrane–bound Qa-SNARE. These observations led us to explore the functional interaction between SEC11 and SYP121 and its potential for regulating secretory traffic at the plant plasma membrane.

Here, we report the binding of SEC11 with SYP121 in vivo, and we elaborate an assay to characterize their interactions in vitro. Through these studies, and mutational analysis of SYP121 and SEC11, we observed that SEC11 binds with SYP121 in a manner that depends in part on conserved residues within the N terminus of the Qa-SNARE and the SM protein, analogous to the patterns of binding reported for mammalian and yeast SM proteins. SEC11 binding with SYP121 was affected by SNAP33 and VAMP721, leading to their apparent competition with the SM protein. Unusually, this competition depended on SEC11 association with the SYP121 N terminus, which, in nonplant models, conversely potentiates interactions between the cognate SNAREs. Thus, while SEC11 binding regulates SYP121 availability for cognate SNARE binding, its interactions leading up to SNARE complex assembly imply a "handshake" or exchange with additional factors in order to trigger complex formation.

RESULTS

SYP121 and SEC11 Interact Directly in Vitro and in Vivo

We optimized in vitro pull-down assays using *Arabidopsis* proteins expressed and purified from *Escherichia coli* (see Supplemental Figure 1 online). For this purpose, the coding sequence for SYP121 was truncated to remove the hydrophobic C-terminal transmembrane domain (SYP121$^{\Delta C}$), yielding the coding sequence for the SYP121-Sp2 fragment previously shown to be active in vivo (Geelen et al., 2002; Sutter et al., 2006b; Tyrrell et al., 2007). A construct was generated to give SYP121$^{\Delta C}$ fused at its C terminus with two Protein-A tags (2PA) as a soluble protein incorporating the N-terminal residues, Habc and H3 (Qa-SNARE motif) α-helices essential for SYP121 function (Figure 1A). The 2PA tag enabled affinity purification of SYP121$^{\Delta C}$ expressed in *E. coli* (see Supplemental Figure 1 online) and immobilization of the purified protein on IgG Sepharose resin. Its placement at the C terminus of the Qa-SNARE fragment also ensured that the tag was removed from the N-terminal end of the protein where it might affect SEC11 interactions (Aran et al., 2009). As controls, we cloned, expressed, and purified 2PA on its own, and the endomembrane Qa-SNARE SYP21 (=PEP12) similarly truncated to give SYP21$^{\Delta C}$ (=SYP21-Sp2) (Tyrrell et al., 2007). As a binding partner, we cloned SEC11 tagged on its N terminus with glutathione *S*-transferase (GST) or 6xHis (=His; Figure 1A; see Supplemental Figure 1 online). For pull-down assays, the baits SYP121$^{\Delta C}$-2PA and 2PA were immobilized on IgG Sepharose and incubated with a fivefold excess of His-SEC11. Thereafter, unbound His-SEC11 was removed by washing and proteins bound to the resin were eluted, separated by SDS-PAGE, and analyzed by immunoblot.

We found that SYP121$^{\Delta C}$-2PA, but not 2PA alone, bound His-SEC11 (Figure 1B) as confirmed with the immunoblot analysis (Figure 1C). Similar results were obtained when the SYP121–SEC11 interaction was tested using the N-terminally tagged GST-SEC11 as the bait for SYP121$^{\Delta C}$-2PA, whereas no significant interaction was observed with the endomembrane Qa-SNARE fusion SYP21$^{\Delta C}$-2PA nor when resin alone was used for

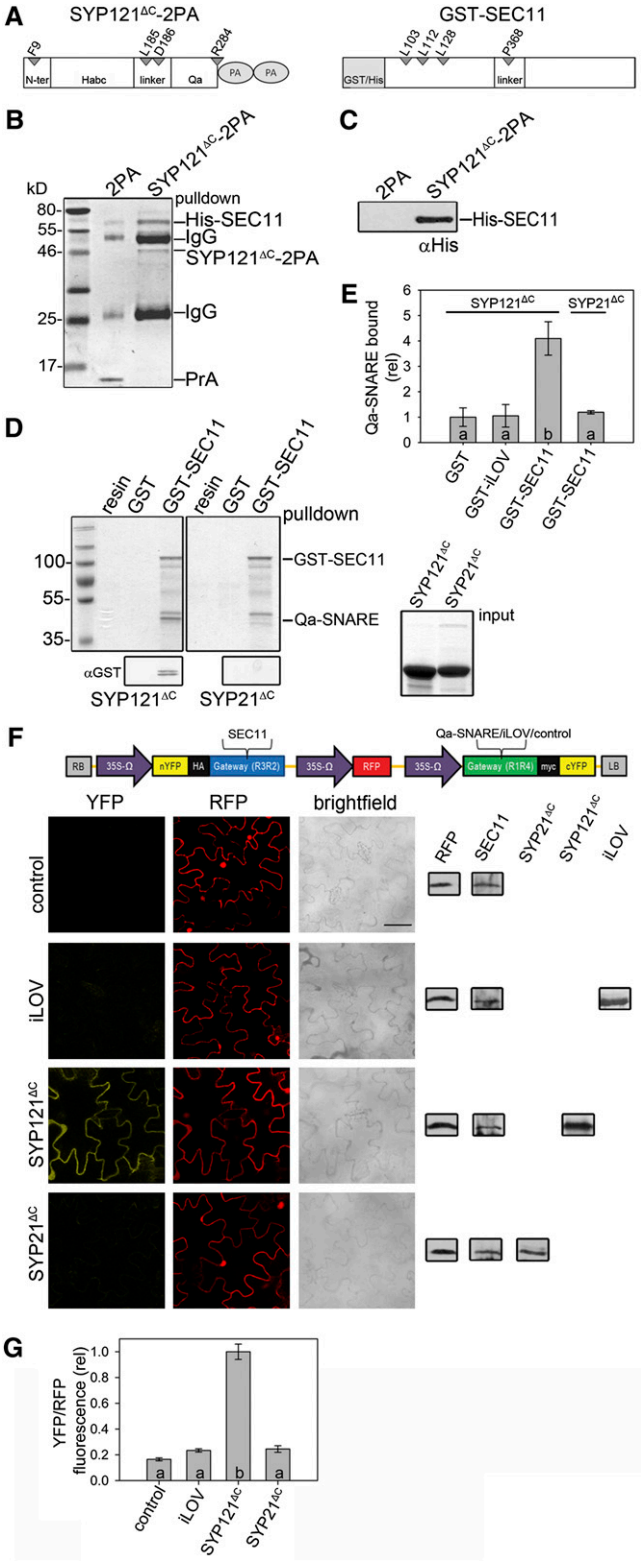

Figure 1. SYP121 and SEC11 Interact Selectively in Vitro and in Vivo.

(A) Schematics of the tagged SYP121$^{\Delta C}$ and SEC11 constructs used in the study. Positions of key residues are as indicated. SEC11 was tagged N-terminally with either GST or with 6xHis residues.

pull-down controls (Figure 1D). Figure 1E summarizes the pull-down data from five independent experiments. Experiments with GST-tagged iLOV protein (GST-iLOV) as bait also showed no significant binding above GST alone (see Supplemental Figure 2 online). iLOV is an unrelated, phototropin protein that is soluble and expressed constitutively in *Arabidopsis* (Chapman et al., 2008). We quantified the corresponding SDS-PAGE bands after Coomassie staining, using ImageJ to derive density ratios for SYP121$^{\Delta C}$-2PA bound as a function of bait input, and the relative SYP121$^{\Delta C}$-2PA binding between baits. The analysis shows that GST alone and GST-iLOV bound similar amounts of SYP121$^{\Delta C}$-2PA, whereas SYP121$^{\Delta C}$-2PA bound to GST-SEC11 was roughly fourfold higher. SYP21$^{\Delta C}$-2PA bound with GST-SEC11 was similar to the background with GST alone.

To assess SYP121 binding with SEC11 in vivo, we cloned the same coding sequences into the 2in1 vector system (Grefen and Blatt, 2012) for transient transformation, expression, and ratiometric bimolecular fluorescence complementation (rBiFC). We made use of the SYP121$^{\Delta C}$ backbone tagged at its C terminus because the C terminus of the full-length Qa-SNARE is not

(B) Coomassie-stained gel of the eluted bait and prey proteins. 2PA and SYP121$^{\Delta C}$-2PA were used as baits in pull-down assays with 6His-SEC11. Loading was adjusted to give equivalent amounts of baits in each lane and pull downs were performed with fivefold excess of prey.

(C) Immunoblot analysis of SEC11 bound in **(B)** using αHis antibody.

(D) Coomassie-stained gels showing proteins recovered in pull-down assays with SYP121$^{\Delta C}$-2PA and SYP21$^{\Delta C}$-2PA using GST and GST-SEC11 as baits. Lanes are (left to right) the molecular weight marker; SYP121$^{\Delta C}$-2PA pull down with resin only, with GST, and with GST-SEC11; and SYP21$^{\Delta C}$-2PA pull-down with resin only, with GST, and with GST-SEC11. GST-SEC11 and Qa-SNARE bands are indicated on the right. Immunoblots probed with αGST antibody in the GST and GST-SEC11 lanes (bottom) show the presence of SYP121$^{\Delta C}$ only in the pull downs. Pull downs were performed with fivefold excess of Qa-SNARE protein. Note that SYP121 yields a doublet band (Leyman et al., 1999; Geelen et al., 2002). Aliquots of the Qa-SNARE inputs for the pull-down assays are shown separately (right).

(E) Relative Qa-SNARE binding normalized against the corresponding proteins bound with GST alone. Data are means ± SE of five independent experiments. Significance of differences indicated by letters ($P < 0.007$). See also Supplemental Figure 2 online.

(F) rBiFC images collected from tobacco transformed using the pBiFCt-2in1-NC (Grefen and Blatt, 2012) tricistronic vector (schematic above). Images are (left to right) YFP (BiFC) fluorescence, RFP fluorescence as a cell marker, and bright-field. Constructs included coding sequences for nYFP-SEC11 and (top to bottom) either the empty cassette or as X-cYFP fusions with the iLOV protein, SYP121$^{\Delta C}$, and SYP21$^{\Delta C}$. Bar = 30 μm. Immunoblot analysis verifying the expression of the fusion proteins and RFP marker are included (right). SEC11 was detected using αSEC11 antibody (Assaad et al., 2001); SYP121$^{\Delta C}$ and SYP21$^{\Delta C}$ were detected using αSYP121 and αSYP21 antibodies (Tyrrell et al., 2007), respectively; and iLOV and RFP were detected using αRFP antibody.

(G) Means ± SE of rBiFC data from four independent experiments, each with 30 images taken at positions selected at random over the leaf surface. rBiFC fluorescence ratios were calculated from the mean fluorescence intensities determined from each YFP/RFP image pair after background subtraction. Significance of difference is indicated by letters ($P < 0.002$).

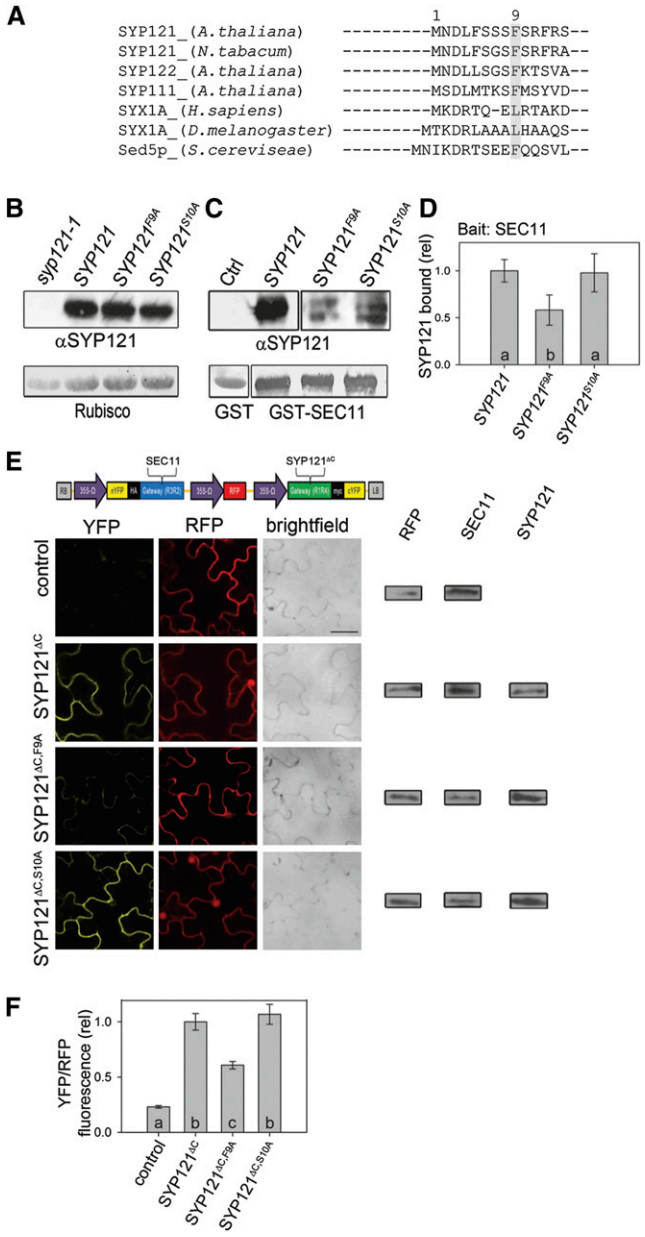

Figure 2. The Conserved Phe Residue at Position 9 of SYP121 Is Important for SEC11 Interaction.

(A) Alignment of the N terminus of SYP121 and related Qa-SNAREs from *Arabidopsis* and tobacco with plasma membrane Qa-SNAREs from human, *Drosophila*, and the Golgi Qa-SNARE of *Saccharomyces cerevisiae*.
(B) Immunoblot analysis of membrane fractions used as inputs for pull-down assays and isolated from the *Arabidopsis syp121-1* mutant and the *syp121-1* mutant complemented with wild-type *SYP121* and with the mutants *SYP121*^{F9A} and *SYP121*^{S10A}. Ponceau-stained ribulose-1,5-bis-phosphate carboxylase/oxygenase (Rubisco) bands are included as a loading control (bottom).
(C) Immunoblot analysis of SYP121 recovered in pull-down assays using GST and GST-SEC11 as baits. Lanes 1 and 2 are pull downs of fractions from *SYP121*-complemented *syp121-1* mutant plants using GST alone and GST-SEC11, respectively. Ponceau-stained GST and GST-SEC11 bands are included as a loading control (bottom). SYP121 was detected with αSYP121 antibody (Tyrrell et al., 2007).

cytosolic and an N-terminal tag might interfere with SEC11 binding. The 2in1 system incorporates a set of independent Gateway-compatible cassettes with 35S promoters (Figure 1F, schematic). The two cassettes include the coding sequences for the two halves of yellow fluorescent protein (YFP), nYFP and cYFP, to generate fusion constructs for coexpression and testing of fluorescence complementation in the plant. The vector also includes a third cassette incorporating the coding sequence for soluble red fluorescent protein (RFP) that can be used, on a cell-by-cell basis, as an expression control and for ratiometric quantification of BiFC. We performed transient transformations of tobacco (*Nicotiana tabacum*) leaves in four independent experiments, each with 2in1 vectors carrying constructs for SEC11 expression alone, with iLOV, with SYP121$^{\Delta C}$, and with SYP21$^{\Delta C}$. Fluorescence was measured by confocal microscopy in each case, and rBiFC data were determined by analysis of images of the epidermal cell layer taken from regions selected at random across the leaf surface. Representative images are shown in Figure 1F along with protein blot analysis for construct expression from the tissue as a whole, and the statistical analysis from all four experiments is summarized in Figure 1G. Much as in the in vitro binding assays, we observed a highly significant rBiFC signal when SEC11 was coexpressed with SYP121$^{\Delta C}$ compared with that obtained with SEC11 expression alone, whereas coexpression with iLOV and with SYP21$^{\Delta C}$ yielded rBiFC signals that were statistically indistinguishable from this background. Thus, both in vitro and in vivo, the results indicated a selective affinity for binding between the *Arabidopsis* SYP121 and SEC11 proteins.

The N Terminus of SYP121 Affects Its Binding with SEC11

The N-terminal peptides of a number of Qa-SNAREs from mammals, yeast, and *Drosophila melanogaster* harbor a set of highly conserved residues, notably Phe (or Leu) at position 8 or 9, that are known to contribute to SM protein binding (Bracher and

(D) SYP121 bound in **(C)** and other experiments as a fraction of the GST-SEC11 bait input and normalized between experiments to data for *SYP121* wild-type complementation after background subtraction. Data are means ± SE of $n = 4$ experiments. Significance of difference is indicated by letters ($P < 0.01$).
(E) rBiFC images collected from tobacco transformed using the pBiFCt-2in1-NC (Grefen and Blatt, 2012) tricistronic vector (schematic above). Images are (left to right) YFP (BiFC) fluorescence, RFP fluorescence as a cell marker, and bright-field. Constructs included coding sequences for nYFP-SEC11 and (top to bottom) either the empty cassette (control) or, as X-cYFP fusions, the SYP121$^{\Delta C}$ and the mutants SYP121$^{\Delta CF9A}$ and SYP121$^{\Delta CS10A}$. Bar = 30 μm. Protein gel blot analysis verifying expression of the fusion proteins and RFP marker are shown (right). SEC11 was detected using αSEC11 antibody (Assaad et al., 2001), SYP121 constructs were detected using αSYP121 antibody (Tyrrell et al., 2007), and RFP was detected using αRFP antibody.
(F) Means ± SE of rBiFC data from four independent experiments, each with 30 images taken at positions selected at random over the leaf surface. rBiFC fluorescence ratios were calculated from the mean fluorescence intensities determined from each YFP/RFP image pair after background subtraction. Significance of difference is indicated by letters ($P < 0.005$).

Weissenhorn, 2002; Dulubova et al., 2002; Burgoyne and Morgan, 2007; Honsbein et al., 2011). Alignment of these Qa-SNAREs with SYP121, with its closest homologs SYP122 and SYP111 from *Arabidopsis* and with SYP121 from tobacco (Figure 2A), showed a similar conservation of the Phe residue at position 9 in the plant Qa-SNAREs. To test its role in binding SEC11 in vivo, and thus with a full complement of associated regulatory factors, we generated transgenic *Arabidopsis* in the *syp121-1* mutant background (Collins et al., 2003), complementing the mutation with the wild-type Qa-SNARE and with SYP121 mutated to carry the site substitutions F9A ($SYP121^{F9A}$); as a control, we included a second, adjacent site complementation with S10A ($SYP121^{S10A}$) (Grefen et al., 2010a). Expression of the Qa-SNARE in each of the complemented lines was verified by immunoblot. We performed pull-down assays using solubilized membrane fractions from leaves of each line with resin-bound GST-SEC11 as the bait. As a control, GST was added with membrane fractions from SYP121-complemented *syp121-1* mutant plants. After washing, bait and bound proteins were eluted, separated as before, and visualized by immunoblotting with polyclonal anti-SYP121 antibody (Tyrrell et al. 2007).

Figure 2B (top) shows the immunoblot for the *syp121-1* mutant background and for the Qa-SNARE inputs used in the pull-down assays; the Ponceau-stained bands for ribulose-1,5-bis-phosphate carboxylase/oxygenase (bottom) are provided as a loading control. Figure 2C (top, left to right) shows the SYP121 pull downs from fractions of *SYP121*-complemented plants using GST (Ctrl) and GST-SEC11 (*SYP121*) as baits and with GST-SEC11 from $SYP121^{F9A}$ and $SYP121^{S10A}$ complemented *syp121-1* mutant plants; the corresponding Ponceau-stained bands for the GST and GST-SEC11 baits are included for reference (bottom). These results demonstrated the lack of binding with GST alone with fractions from the *SYP121*-complemented *syp121-1* mutant. They also indicated SYP121 binding with SEC11 in the other samples, albeit visibly reduced in fractions from the $SYP121^{F9A}$-complemented plants. In each case, SYP121 could be resolved as a double band in the eluted fraction, consistent with previous observations (Geelen et al., 2002; Tyrrell et al., 2007). Band intensities were quantified using ImageJ and relative binding determined from the ratios of Qa-SNARE bound against GST-SEC11 input. Figure 2D summarizes the results from four independent experiments with binding normalized between experiments to binding for the *SYP121*-complemented plants. The analysis confirms that SYP121 binding to SEC11 was significantly reduced by the F9A mutation, but not by the S10A mutation.

We examined the SEC11 interaction with SYP121 in vivo, again taking advantage of the 2in1 system for rBiFC (Grefen and Blatt, 2012). rBiFC fusion constructs (Figure 2E, schematic) were generated to express nYFP-SEC11 together with cYFP fusions of wild-type $SYP121^{\Delta C}$, $SYP121^{\Delta C,F9A}$, and $SYP121^{\Delta C,S10A}$ and with RFP as the expression marker. Figure 2E shows confocal fluorescence images collected for each of the Qa-SNARE constructs and for the SEC11 control after transient transformation of tobacco leaves along with protein blot analysis verifying expression in the whole tissue. Analysis of the fluorescence intensity ratios for four independent experiments is summarized in Figure 2F. These results support the pull downs from *Arabidopsis* microsomal fractions; they show that SEC11 interacts selectively with SYP121 in vivo and that its binding is sensitive to the Phe residue at position 9 of the Qa-SNARE.

Probing SEC11 Binding with SYP121

Many Qa-SNAREs have been shown to adopt two alternative conformations: (1) a closed conformation in which the three N-terminal α-helices of the Habc domain fold back onto the H3 (Qa motif) α-helix and form a tetrahelical bundle, and (2) an open conformation in which the H3 α-helix is free of the N-terminal α-helices and available for binding with the cognate SNAREs (Sutton et al., 1998; Margittai et al., 2003). The open conformation can be stabilized experimentally by introducing point mutations in the linker between the Habc and H3 α-helices, which disrupt binding of the mammalian SM protein Munc18-1 to the closed Syn1A (Dulubova et al., 1999). By contrast, homologous substitutions in the *Arabidopsis* SYP111, which lead to a significant increase in trypsin proteolysis consistent with a more open structure, increase in its binding to SEC11 (Park et al., 2012). We found that introducing the corresponding substitutions to yield $SYP121^{\Delta C,L185A,D186A}$ also increased the binding in pull downs with GST-SEC11 (Figures 3A and 3B). However, unlike the N-terminal deletion of SYP111 (Park et al., 2012), significant binding was retained with the complementary $SYP121^{\Delta C,L185A,D186A,F9A}$ mutant. These data indicate that SEC11 binding is enhanced with SYP121 in its open conformation, as it is for SYP111. Our observations also suggest that the F9 residue helps to stabilize SEC11 with the Qa-SNARE, consistent with the in vivo data (Figure 2), although it is not indispensable for binding in either the closed or open conformation of SYP121.

SM proteins resolved to date have been found to form a clothespeg-like structure with a central cavity that is thought to clasp the closed conformation of the cognate Qa-SNARE. In the mammalian SM protein Munc18-1, amino acids central to the protein between residues 295 and 358 form a flexible hairpin bend that is required for Qa-SNARE binding; the P335A mutation reduces the flexibility of this hairpin and disrupts binding associated with both the N terminus and closed conformations of the Qa-SNARE Syn1A (Misura et al., 2000; Hu et al., 2011). On its own, the N terminus of the Qa-SNARE connects with a hydrophobic cleft on the outer surface of the SM protein, within its N-terminal leg, to facilitate membrane fusion (Shen et al., 2010). Consistent with this finding, the L117R and L137R mutations of the yeast SM proteins Vps45p and Sly1p prevent their association with the N terminus of the cognate Qa-SNAREs Tlg2p and Sed5p (Peng and Gallwitz, 2004; Carpp et al., 2006). We identified three potentially homologous sites (Figure 3C) and generated mutations in each of these to yield the single-site mutants L103R, L112R, and L128R in addition to the hairpin mutation P368A in GST-SEC11. Pull-down assays with $SYP121^{\Delta C}$ (Figures 3D and 3E) showed that binding was reduced in every case and was most strongly affected by the $SEC11^{L128R}$ and $SEC11^{P368A}$ mutations. Together with the results of Figure 2, these data are broadly consistent with two modes of binding between SEC11 and SYP121, one depending on the interaction of the SYP121 N terminus with the outer surface of SEC11 and the second

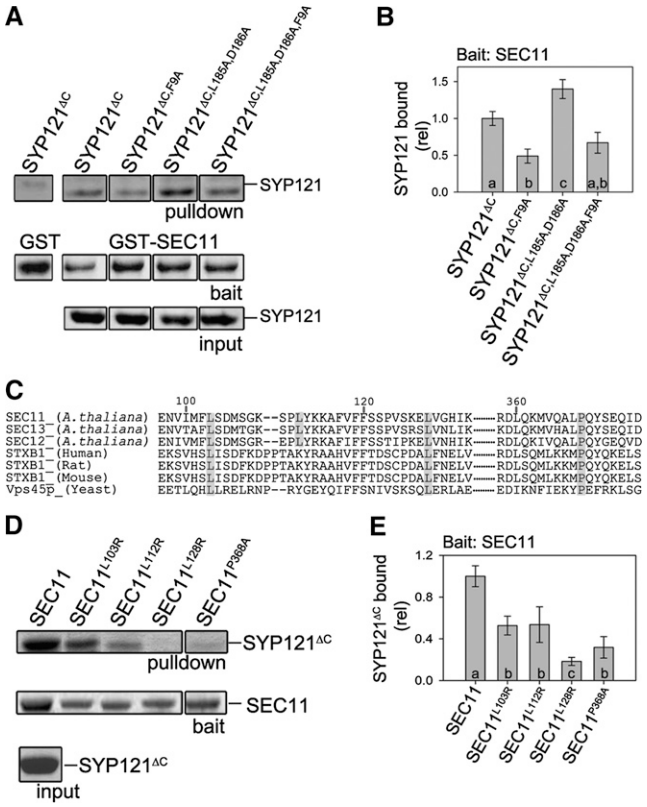

Figure 3. SYP121 Structure and Residues in the N-Terminal Leg of SEC11 Are Essential for Their Binding.

(A) Efficacy in SYP121 pull down with GST-SEC11 as bait. Coomassie-stained gels of the Qa-SNARE forms recovered (top) from the input (bottom) using the bait (center). SYP121 forms are (left to right) SYP121$^{\Delta C}$, SYP121$^{\Delta C,F9A}$, SYP121$^{\Delta C,L185A,D186A}$, and SYP121$^{\Delta C,L185A,D186A,F9A}$. Additional bands (far left) show SYP121$^{\Delta C}$ pull down with GST alone as a control.

(B) Relative binding of the Qa-SNARE forms in **(A)** determined as the fraction bound relative to the GST-SEC11 bait and normalized between experiments to the result for SYP121$^{\Delta C}$ binding after subtracting the background with GST alone. Data are the means ± SE of four independent experiments. Significance of difference is indicated by letters ($P < 0.05$).

(C) Protein sequence alignment of SEC11 with its *Arabidopsis* homologs and selected SM proteins from other eukaryotes in the N-terminal leg and hinge regions. Note the highly conserved Leu residues at positions 103, 112, and 128 and the conserved Pro in the hinge at position 368 (gray highlighting). Numbering refers to SEC11.

(D) Efficacy in SYP121 pull down using GST-SEC11 and the mutants GST-SEC11^{L103R}, GST-SEC11^{L112R}, GST-SEC11^{L128R}, and GST-SEC11^{P368A}. Coomassie-stained gels of SYP121$^{\Delta C}$ recovered (top) from the input (bottom) using the baits (center).

(E) Relative binding of SYP121$^{\Delta C}$ in **(D)** determined as the fraction bound relative to the bait and normalized between experiments to the result for SYP121$^{\Delta C}$ binding with GST-SEC11 after subtracting the background with GST alone (see **[A]**). Data are the means ± SE of four independent experiments. Significance of difference is indicated by letters ($P < 0.008$).

engaging a homologous, clothespeg-like cleft formed by the SM protein.

SEC11 Competes for SYP121 Binding with Its Cognate SNAREs

Although originally associated with the closed conformation of canonical Qa-SNAREs from yeast and mammals (Bracher et al., 2000; Bracher and Weissenhorn, 2002), the binding of SM proteins is recognized now also to facilitate vesicle fusion by stabilizing the complex of cognate SNAREs (Burgoyne and Morgan, 2007; Südhof and Rothman, 2009). SYP121 is known to assemble a SNARE core complex with the Qbc-SNARE SNAP33 and R-SNARE VAMP721 (Kwon et al., 2008), thus raising the question whether SEC11 binding affects (and is affected by) SYP121 interaction with these protein partners. We expressed and purified SNAP33 and the cytosolic domain of VAMP721 tagged with GST as before (see Supplemental Figures 1D and 1E online) for pull-down assays with SYP121$^{\Delta C}$-2PA as bait. Equimolar quantities of VAMP721 and SNAP33 were incubated at a fivefold excess with the Qa-SNARE on their own, together, and with GST-SEC11. After washing, the bound proteins were eluted, separated by SDS-PAGE, and analyzed by immunoblotting with anti-GST antibody. We found that GST-SNAP33 and GST-VAMP721 bound similarly when added either alone or together with the complementary Qa-SNARE partner (Figures 4A to 4C). The observations indicated the ability of the proteins to assemble in heteromeric complexes with all three cognate SNAREs and suggested a dynamic between the closed and open conformations of the Qa-SNARE sufficient to allow this assembly (contrast with mammalian Syn1A; Calakos et al., 1994).

In subsequent experiments, we incubated GST-SEC11 with SYP121$^{\Delta C}$ in sequence, adding the SM protein before, after, or at the same time as GST-SNAP33 and GST-VAMP. Bound proteins were analyzed as before and ratios normalized between experiments to the values obtained when SEC11, SNAP33, and VAMP721 were introduced concurrently in the pull-down assay. Immunoblots from one experiment are shown in Figure 4D, and the results of five independent experiments are summarized for SEC11 and SNAP33 in Figures 4E and 4F. SEC11 bound with SYP121$^{\Delta C}$ was significantly greater when present on its own and was further enhanced when incubated first with SYP121$^{\Delta C}$ before adding the cognate SNAREs VAMP721 and SNAP33; no difference in SEC11 binding was evident when added together with or after VAMP721 and SNAP33 (Figure 4E). SNAP33 binding with SYP121$^{\Delta C}$ was also significantly greater in the absence of SEC11 (Figure 4F). When compared with the results of the concurrent additions, SNAP33 binding was unaffected when SEC11 was incubated first with SYP121$^{\Delta C}$, but its binding was enhanced if SEC11 was added after SYP121$^{\Delta C}$ was incubated with SNAP33 and VAMP721 (Figure 4F). A simple interpretation of these data is that SEC11 and SNAP33 compete for the unbound SYP121, but assembly of the SNARE core complex facilitates SEC11 binding, which, once bound, also helps stabilize the association of SYP121 with SNAP33.

As a test of this hypothesis, we repeated these experiments using the SYP121$^{\Delta C,L185A,D186A}$ mutant as bait, with the expectation that locking the Qa-SNARE in the open conformation

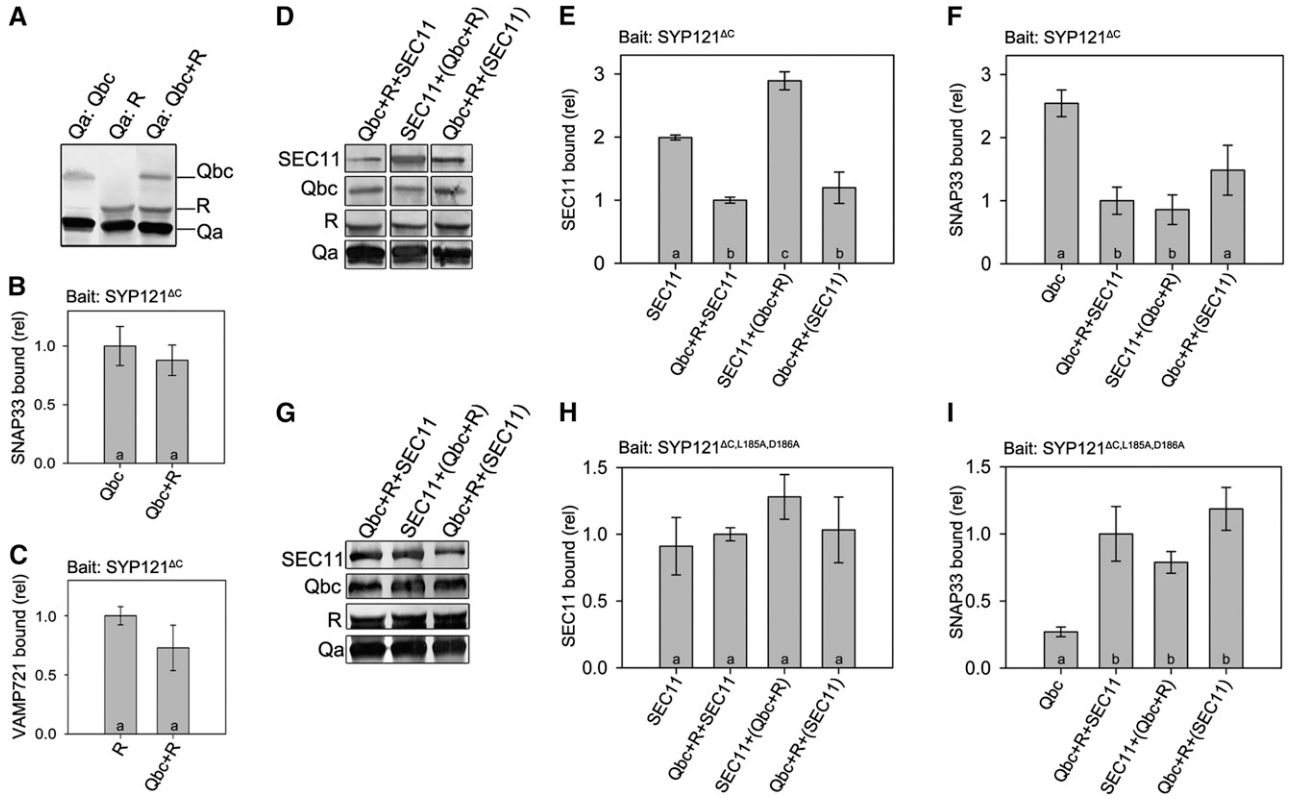

Figure 4. SEC11 Competes with SNAP33 and VAMP721 for SYP121$^{\Delta C}$ Binding, but Not for Binding with SYP121$^{\Delta C,L185A,D186A}$.

(A) Immunoblot analysis of pull downs showing GST-SNAP33 and GST-VAMP721 recovered with SYP121$^{\Delta C}$-2PA as the bait. The Qa-SNARE partners were added in fivefold excess and incubated individually and together along with SYP121$^{\Delta C}$-2PA. Bands were resolved from a single gel using αGST antibody and SYP121$^{\Delta C}$-2PA detected by binding of the IgG to Protein A. Labels here and elsewhere are for simplicity: Qa (=SYP121$^{\Delta C}$-2PA), Qbc (=GST-SNAP33), and R (=GST-VAMP721).

(B) and **(C)** Relative binding of GST-SNAP33 **(B)** and GST-VAMP721 **(C)** with SYP121$^{\Delta C}$-2PA from five independent experiments including the data in **(A)**. Data are means ± SE and have been normalized between experiments to the means for binding in the dimeric incubations. Significance of difference is indicated by letters ($P < 0.05$).

(D) Immunoblot analysis of pull downs with SYP121$^{\Delta C}$-2PA as bait in the presence of SEC11. Incubations were performed adding GST-SEC11 together (=Qbc+R+SEC11), before [=SEC11+(Qbc+R)], and after [=Qbc+R+(SEC11)] preincubation with GST-SNAP33 and GST-VAMP721. Equimolar GST-SEC11, GST-SNAP33, and GST-VAMP721 were added in each case and in fivefold excess to the SYP121$^{\Delta C}$-2PA bait. Results of parallel dimeric incubations with GST-SEC11 alone (see also Figures 1 to 3) are included in **(E)** and **(F)**.

(E) and **(F)** Relative binding of GST-SEC11 **(E)** and GST-SNAP33 **(F)** with SYP121$^{\Delta C}$-2PA from five independent experiments including the data in **(D)**. Data are means ± SE and have been normalized between experiments to the means for the tetrameric incubations with all proteins added simultaneously. Significance of differences indicated by letters ($P < 0.02$).

(G) Immunoblot analysis of pull downs with SYP121$^{\Delta C,L185A,D186A}$-2PA as bait in the presence of SEC11. Incubations were performed adding GST-SEC11 together (=Qbc+R+SEC11), before [=SEC11+(Qbc+R)], and after [=Qbc+R+(SEC11)] preincubation with GST-SNAP33 and GST-VAMP721. Equimolar GST-SEC11, GST-SNAP33, and GST-VAMP721 were added in each case and in fivefold excess to the SYP121$^{\Delta C,L185A,D186A}$-2PA bait. Results of parallel dimeric incubations with GST-SEC11 alone (see also Figures 1 to 3) are included in **(H)** and **(I)**.

(H) and **(I)** Relative binding of GST-SEC11 **(H)** and GST-SNAP33 **(I)** with SYP121$^{\Delta C,L185A,D186A}$-2PA from four independent experiments including the data in **(G)**. Data are means ± SE and have been normalized between experiments to the means for the tetrameric incubations with all proteins added simultaneously. Significance of difference is indicated by letters ($P < 0.02$).

would eliminate the competition for binding between SEC11 and the cognate SNARE partners. The results, summarized in Figures 4G to 4I, confirmed that SEC11 binding to SYP121$^{\Delta C,L185A,D186A}$ was unaffected by additions of the cognate SNAREs and independent of the order of additions (Figure 4H). Furthermore, adding SEC11 led to a significant increase in SNAP33 binding with SYP121$^{\Delta C,L185A,D186A}$, again independent of the order of additions (Figure 4I). These results, and those of Figures 2 and 3, are most easily understood in context of the two conformations of SYP121, both available for SEC11 binding: When presented with the open conformation of the SYP121$^{\Delta C,L185A,D186A}$ mutant and with the cognate SNAREs, SEC11 is able to bind and stabilize the core complex; when bound in the closed conformation, SEC11 sequesters SYP121, effectively competing out the Qa-SNARE for binding, even with its cognate SNARE partners.

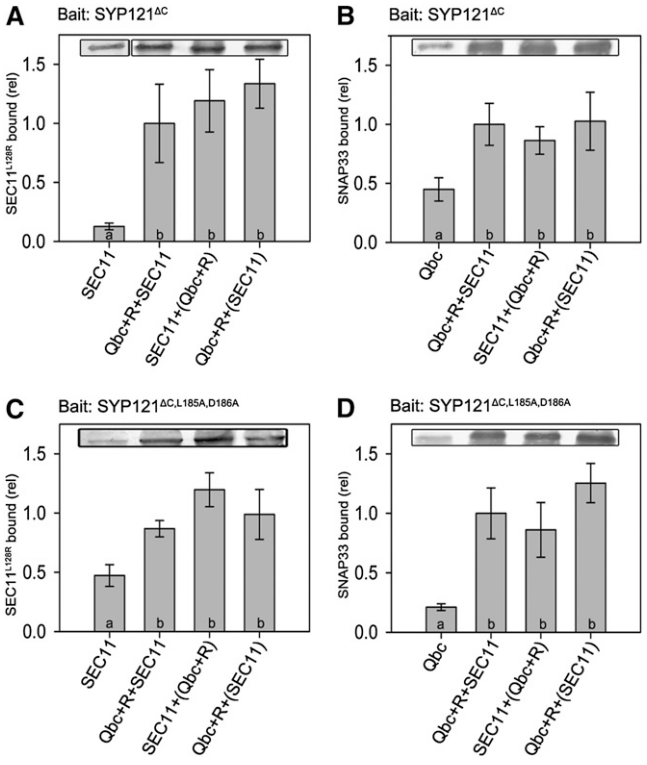

Figure 5. SEC11^{L128R} Binding to SYP121$^{\Delta C}$ and to SYP121$^{\Delta C,L185A,D186A}$ Is Enhanced by SNAP33 and VAMP721.

Experiments were performed with ordered additions of GST-SEC11^{L128R}, GST-SNAP33, and GST-VAMP721 as in Figure 4. Labels are for simplicity: Qbc (=GST-SNAP33) and R (=GST-VAMP721). Incubations were performed with GST-SEC11^{L128R} added together (=Qbc+R+SEC11), before [=SEC11+(Qbc+R)], and after [=Qbc+R+(SEC11)] preincubation with GST-SNAP33 and GST-VAMP721. Data are means ± SE of five independent experiments and have been normalized between experiments to the means for the tetrameric incubations with all proteins added simultaneously. Significance of difference is indicated by letters ($P < 0.05$).

(A) and **(B)** Relative binding of GST-SEC11^{L128R} **(A)** and GST-SNAP33 **(B)** with SYP121$^{\Delta C}$-2PA. Insets: Immunoblot analysis for GST-SEC11^{L128R} **(A)** and GST-SNAP33 **(B)** from one experiment in each case.

(C) and **(D)** Relative binding of GST-SEC11^{L128R} **(C)** and GST-SNAP33 **(D)** with SYP121$^{\Delta C,L185A,D186A}$-2PA. Insets: Immunoblot analysis for GST-SEC11^{L128R} **(C)** and GST-SNAP33 **(D)** from one experiment in each case.

SEC11 Interaction with the SYP121 N Terminus Facilitates Competitive SNARE Binding

Binding of SM proteins with the N terminus of the cognate Qa-SNAREs is thought variously to stabilize their interactions (Carpp et al., 2006; Dulubova et al., 2007; Khvotchev et al., 2007) and to tether and potentiate SNARE complex assembly in the presence of the cognate SNAREs (Tareste et al., 2008; Rathore et al., 2010). Thus, we were interested that SEC11 appeared to compete for SYP121 binding with its cognate SNAREs and that this competition was eliminated when presented with the open conformer SYP121$^{\Delta C,L185A,D186A}$. To explore the role of this association further, we made use of the SEC11^{L128R} mutant that largely eliminated binding with SYP121$^{\Delta C}$ alone (Figures 3D and 3E). We reasoned that if interaction with the SYP121 N terminus was important for SEC11 competition with the cognate SNAREs, then the mutation should eliminate this competition by preventing SEC11 association with the SYP121 N terminus. Pull-down assays were performed as before, but with the substitution of the SEC11^{L128R} mutant. We found SEC11^{L128R} binding to be strongly enhanced when SNAP33 and VAMP721 were present, but independent of the order of incubation with SYP121$^{\Delta C,L185A,D186A}$ (Figure 5A). SNAP33 binding was enhanced by SEC11^{L128R}, again independent of the order of additions (Figure 5B), consistent with the loss of SM protein binding to the closed Qa-SNARE (compared with Figures 3 and 4). Similar results were obtained when the open conformation mutant SYP121$^{\Delta C,F9A,L185A,D186A}$ was used as bait (Figures 5C and 5D), which also suggests that binding with the N terminus of the Qa-SNARE is not essential for priming SNARE core complex assembly with SYP121.

Finally, to assess SYP121$^{\Delta C}$ and SYP121$^{\Delta C,L185A,D186A}$ binding with SEC11 and SEC11^{L128R} in vivo, we cloned the same coding sequences into the 2in1 vector system (Grefen and Blatt, 2012) for transient, 35S-driven expression in tobacco and rBiFC analysis. Confocal images were collected at random across the leaf surface in each of five independent experiments. These data along with protein blot analysis for whole-tissue expression (Figure 6A) and statistical analysis of data from all experiments (Figure 6B) showed that the interaction of SYP121$^{\Delta C,L185A,D186A}$ with SEC11 was only marginally reduced compared with that of SYP121$^{\Delta C}$ but was virtually lost when SEC11^{L128R} was substituted for SEC11. We also noted a smaller, but significant, recovery of the rBiFC signal when SEC11^{L128R} was coexpressed with the open Qa-SNARE SYP121$^{\Delta C,L185A,D186A}$. This recovery may reflect the ability of the tobacco SNAP33 and VAMP721 homologs to assemble with SYP121 (Kargul et al., 2001; Sutter et al., 2006b; Tyrrell et al., 2007), thereby promoting SEC11 binding with the core complex (Figure 5). Thus, we conclude that SEC11 interaction with the SYP121 N terminus is important for their association in vivo and for SEC11 competition with SNAP33 and VAMP721 in SYP121 binding in vitro.

SEC11 Rescues Vesicle Traffic Block by the Dominant-Negative SYP121$^{\Delta C}$

Previous studies (Geelen et al., 2002; Sutter et al., 2006b; Tyrrell et al., 2007) have highlighted the efficacy of SYP121$^{\Delta C}$, the so-called Sp2 fragment of SYP121, to selectively block secretory traffic to the plasma membrane. Traffic block is thought to occur because the soluble SYP121$^{\Delta C}$ retains its ability to assemble in complex with its cognate SNAREs but, lacking a membrane anchor, is unable to facilitate fusion. In short, SYP121$^{\Delta C}$ acts as a dominant-negative inhibitor by competing with the native Qa-SNAREs for binding partners. Therefore, we reasoned that SEC11 might rescue traffic in vivo in the presence of SYP121$^{\Delta C}$, provided that SEC11 binding could stabilize the Qa-SNARE fragment in its closed conformation.

To test this hypothesis, we recloned the coding sequences for SYP121$^{\Delta C}$, SEC11, SEC11^{L128R}, and, as a control, the coding sequence for SYP21$^{\Delta C}$ in the tetracistronic vector pTEcG-2in1-CC

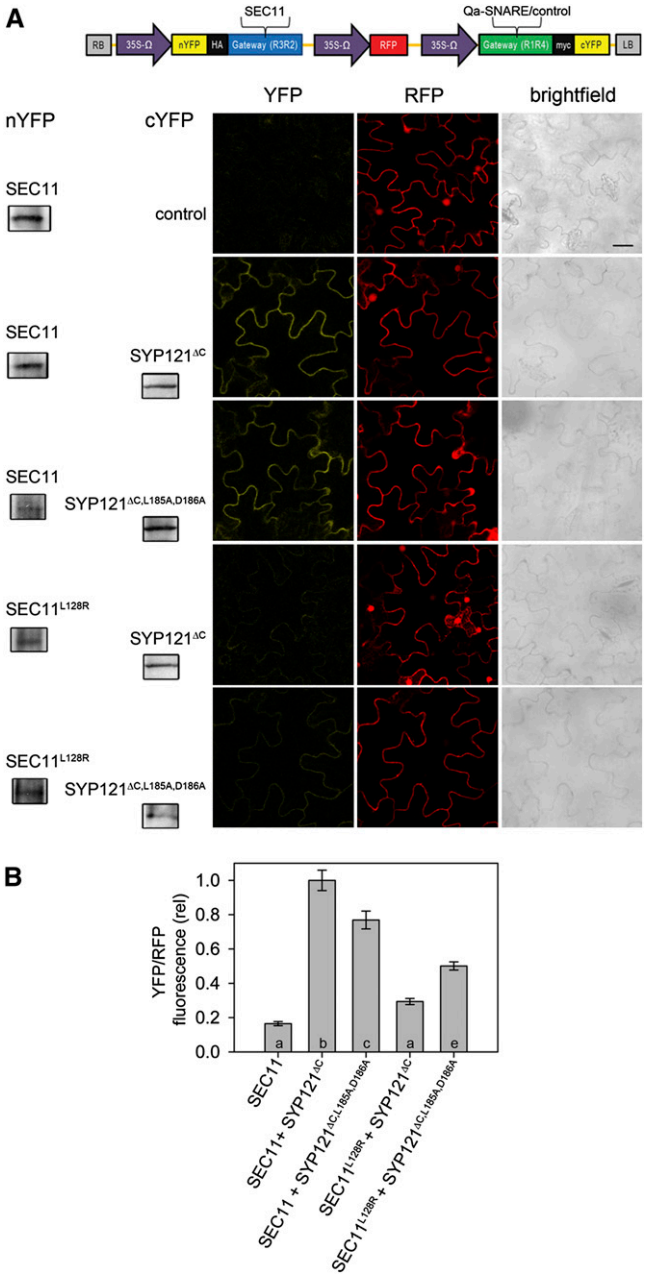

Figure 6. SEC11 Binding to SYP121 in Vivo Is Suppressed by the L128R Site Mutation.

rBiFC analysis of nYFP fusions of SEC11 and SEC11^{L128R} and their interaction with SYP121$^{\Delta C}$ and SYP121$^{\Delta C,L185A,D186A}$.

(A) rBiFC images collected from tobacco transformed using the pBiFCt-2in1-NC tricistronic vector (schematic above). Images are (left to right) YFP (BiFC) fluorescence, RFP fluorescence as a cell marker, and brightfield. Constructs (top to bottom) included coding sequences for nYFP-SEC11 and nYFP-SEC11^{L128R} with either the empty cassette (control) or X-cYFP fusions with SYP121$^{\Delta C}$ and SYP121$^{\Delta C,L185A,D186A}$. Images for SEC11^{L128R} alone were similar to those for SEC11 and have been omitted for simplicity. Bar = 40 μm. Immunoblot analysis verifying expression of the fusion proteins and RFP marker as indicated (left). Expression of fusion constructs SEC11 and SEC11^{L128R} was detected using αSEC11 antibody (Assaad et al., 2001), of SYP121$^{\Delta C}$ and SYP121$^{\Delta C,L185A,D186A}$ using αSYP121 antibody (Tyrrell et al., 2007), and of RFP using αRFP antibody.

(B) Means ± SE of rBiFC data from five independent experiments, each with 30 images taken at positions selected at random over the leaf surface including the images in **(A)**. rBiFC fluorescence ratios were calculated from the mean fluorescence intensities determined from each YFP/RFP image pair after background subtraction. Significance of difference is indicated by letters ($P < 0.02$).

(see Methods). Analogous to the 2in1 system, this vector incorporates four 35S-driven expression cassettes, two containing the coding sequences for expression of the endoplasmic reticulum marker green fluorescent protein (GFP)-HDEL (Boevink et al., 1998; Geelen et al., 2002) and of secreted YFP (secYFP) (Geelen et al., 2002; Tyrrell et al., 2007), respectively, and two available for recombination with Gateway-compatible donor constructs. Transformation with this vector thus ensured equal transgene dosage on a cell-by-cell basis and included a marker for *Agrobacterium tumefaciens*–mediated gene transfer. As with rBiFC (Figures 1 and 6), we used ratiometric analysis of concurrent secYFP and GFP-HDEL fluorescence images to quantify secretory traffic and its block. Figure 7 summarizes the results of four independent experiments with confocal images collected at random across the leaf surface for each construct. We found, as before (Tyrrell et al., 2007), that expressing SYP121$^{\Delta C}$, but not SYP21$^{\Delta C}$, led to a significant block of traffic and retention of the secYFP signal relative to the cellular marker GFP-HDEL. Expressing SEC11 on its own did not lead to secYFP retention, nor did SEC11^{L128R}. However, when coexpressed with SYP121$^{\Delta C}$, SEC11 rescued secYFP traffic, as evidenced by its lack of retention relative to the GFP-HDEL marker. By contrast, coexpressing SEC11^{L128R} with SYP121$^{\Delta C}$ failed to prevent secYFP retention and, hence, to rescue its traffic. These results indicated that SEC11 is able to affect secretory traffic in vivo. We suspect that traffic rescue depends on SEC11 interaction with the dominant-negative Qa-SNARE because the SEC11^{L128R} mutant was unable to rescue traffic, while expression of the native SEC11 alone had no effect. We return to these observations below.

DISCUSSION

SM proteins interact with SNAREs through a complex sequence of binding steps. These interactions regulate vesicle fusion, protecting the cognate Qa-SNARE against promiscuous associations, targeting SNARE complex assembly within the cell and accelerating vesicle fusion by stabilizing the assembled core complex (Burgoyne and Morgan, 2007; Südhof and Rothman, 2009). Although a widely accepted, unifying hypothesis for the precise function(s) of SM proteins remains elusive, common themes have emerged. Notably, SM binding alternates between roles in protecting against promiscuous SNARE interactions through binding with the closed conformation of the Qa-SNARE and in stabilizing cognate SNARE assembly with the open Qa-SNARE to promote vesicle fusion. Furthermore, passage from the first

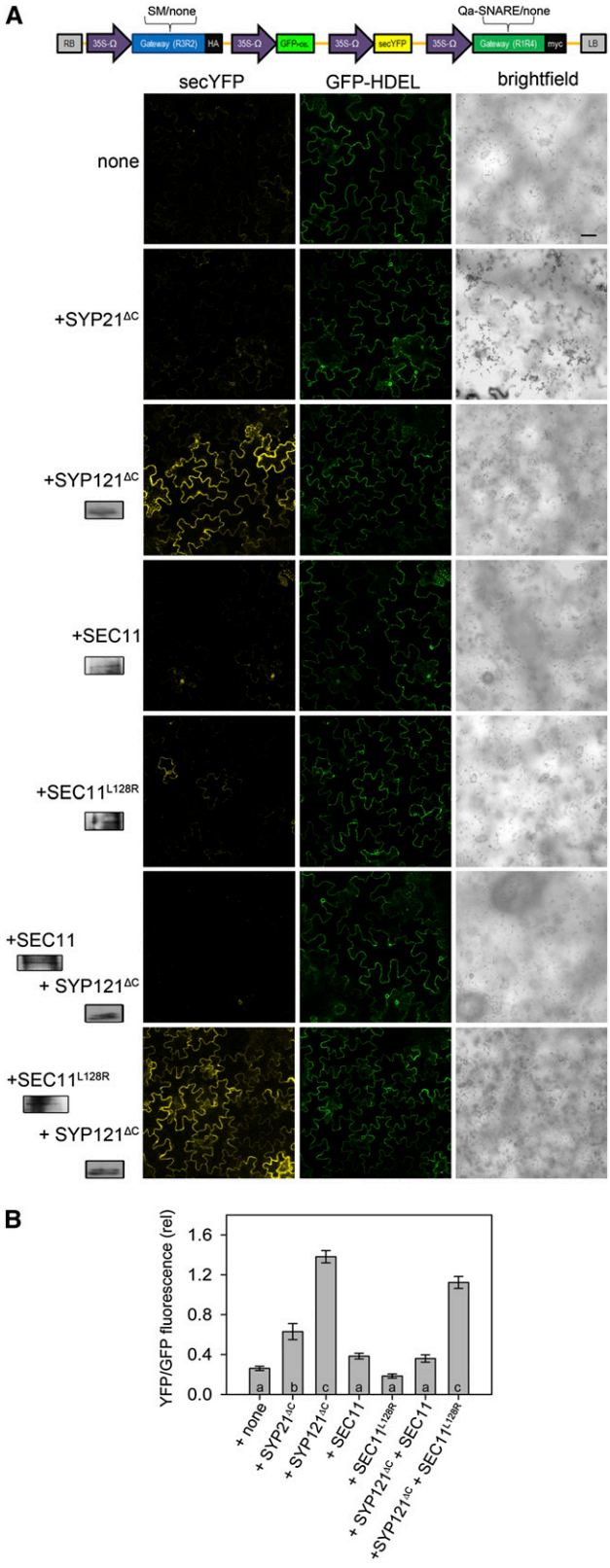

Figure 7. Secretory Traffic Block in Vivo by SYP121$^{\Delta C}$ Is Rescued by SEC11, but Not by SEC11^{L128R}.

to the second of these activities is a concerted process that includes SM tethering to the Qa-SNARE N terminus. An understanding of SM function has been driven by work on mammalian and yeast cell models. Little is known of SNARE dynamics, let alone their relationship to SM proteins in plants. Recent studies (Park et al., 2012) have suggested SM protein binding atypical of these established norms, but in cell plate formation, which may be more closely related to homotypic fusion in yeast than to the classic models of heterotypic vesicle fusion characteristic of much of the traffic activity within plant and animal cells.

Work with the *Arabidopsis* SM protein SEC11 presents a number of challenges. Its genetic null is embryo lethal (Assaad et al., 2001), which makes complementation difficult and precludes its physiological analysis. We adapted a set of in vitro binding methods from work with yeast homologs (Carpp et al., 2006; Aran et al., 2009) and in vivo secretory assays to explore the dynamics of heterotypic SNARE interactions that normally occur at the plant plasma membrane. Here, we report that the Qa-SNARE SYP121 (=SYR1/PEN1), a close homolog of SYP111 (=KNOLLE), binds with the SM protein SEC11 (=KEULE) in vivo and in vitro and that their association affects SYP121 interactions with its cognate SNAREs, some aspects of which are previously undocumented in mammalian and yeast cell models. Four key observations distinguish SEC11-SYP121 dynamics: (1) SEC11 binding with SYP121 on its own is enhanced by mutations that favor the open conformation of the Qa-SNARE, and SEC11 binding to both forms is stabilized by association with the SYP121 N terminus; (2) SEC11 competes with SNAP33 and VAMP721 for binding with SYP121; (3) this competition is lost in favor of enhanced SNAP33 binding in a heteromeric SNARE core complex when mutations are introduced to eliminate SEC11 tethering with the N terminus of SYP121; and (4) the same SEC11 mutation precludes its rescue of secretory traffic in vivo. These findings underline the unusual nature of interactions between SEC11 and its cognate Qa-SNAREs, and they suggest a divergence in the regulation of SM protein binding in plants during the transition between the closed and open, fusion-competent conformations of the Qa-SNARE.

(A) Confocal images (left to right) of the secretory marker (secYFP), cellular marker (GFP-HDEL) fluorescence, and bright-field signals from tobacco epidermis after transformation. Transformations were performed with the tetracistronic pTEcG-2in1-CC vector expressing (top to bottom) secYFP and GFP-HDEL alone and together with SYP21$^{\Delta C}$, SYP121$^{\Delta C}$, SEC11, SEC11^{128R}, and SYP121$^{\Delta C}$ with SEC11 and SEC11^{128R}. Bar = 40 μm. Immunoblot analysis verifying expression of the SYP21$^{\Delta C}$ and SEC11 variants as indicated (left). Expression of fusion constructs SEC11 and SEC11^{L128R} was detected using αSEC11 antibody (Assaad et al., 2001),and of SYP121$^{\Delta C}$ using αSYP121 antibody (Tyrrell et al., 2007).

(B) Means ± SE of relative secYFP retention (=YFP fluorescence/GFP fluorescence) as a measure of secretory block. Fluorescence ratios were calculated from the mean fluorescence intensities determined from 30 image pairs collected at random over the leaf surface in each of four independent experiments after correction for background. Significance of difference is indicated by letters ($P < 0.005$).

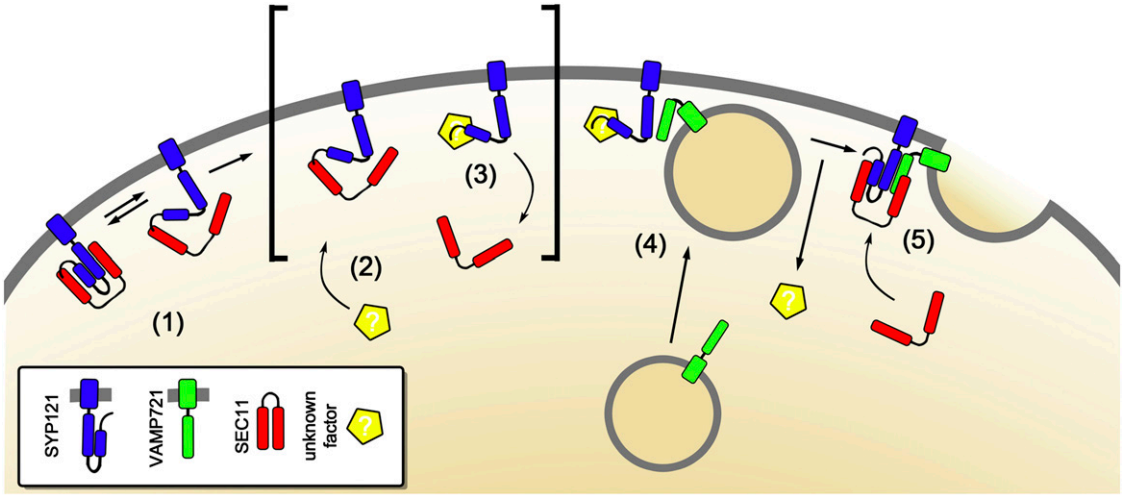

Figure 8. Transition of SEC11 Binding with SYP121 to Facilitate SNARE Complex Formation Is Predicted to Require an Additional Factor That Destabilizes Its Association with the SYP121 N Terminus.

For clarity, only the SNAREs SYP121 and VAMP721 are shown. Binding between the SYP121 N terminus and the N-terminal leg of SEC11 stabilizes the closed state of the Qa-SNARE (1) and must be dislodged by a hypothetical factor (2) to complete the transition to the open, fusion-ready form (3). We speculate that interaction with the cognate SNAREs SNAP33 and VAMP721 releases the hypothetical factor (4), thereby preparing the SNARE complex for binding and stabilization by SEC11 (5) to facilitate vesicle fusion (6). Thus, SEC11-mediated regulation is proposed to rely on a handshaking mechanism of binding-partner exchange.

The SEC11-SYP121 Complex

Maintaining the Qa-SNARE inactive is vital for specificity in vesicle targeting; it is generally consistent with the notion that the SNARE is held by its cognate SM protein in a closed (occluded) conformation and switches to an open, fusion-competent form immediately before vesicle fusion to prevent ectopic SNARE complex assembly. In neurotransmission, the interaction of the SM protein Munc18-1 with the N terminus of the Qa-SNARE Syn1A and the regulatory protein Munc13 (Hughson, 2013; Ma et al., 2013) is important to initiate this switch: Binding with its N terminus releases the Syn1A from the major binding cleft of Munc18-1 and recruits the cognate SNAREs for complex assembly but is not essential for later steps that lead to vesicle fusion (Dulubova et al., 1999; Rathore et al., 2010). Thus, it was unexpected that SEC11 binding with SYP121 alone should be enhanced by mutation of amino acid residues thought to lock the Qa-SNARE in the open conformation and that this binding was suppressed by mutation of the single amino acid at the conserved N-terminal site of the Qa-SNARE (Figures 2 and 3). These findings are largely consistent with SEC11 binding to the SYP121 homolog SYP111 (Park et al., 2012) and were previously interpreted to indicate that the plant SM protein stabilizes the open, fusion-competent form of both Qa-SNAREs. We noted a significant residual binding with the F9A mutant of SYP121 in vivo and, in vitro, both to the wild-type and open forms of SYP121. Thus, we cannot rule out an association with other residues of the N terminus of SYP121. Indeed, Park et al. (2012) eliminated all specific binding on deleting all of the SYP111 N terminus but recovered part of this binding activity when the N-terminal 42 residues of SYP111 were replaced with the first 20 residues of the endomembrane Qa-SNARE SYP21 (=PEP12). We also note below that SEC11 competes for SYP121 binding with its cognate SNARE partners so long as SEC11 is able to interact with the SYP121 N terminus. Thus, the interpretation that SEC11 stabilizes the open conformation of the Qa-SNARE is clearly too simplistic.

Interaction with SYP121 alone was strongly reduced by the single-site mutations SEC11^{L103R} and SEC11^{L112R} and was virtually lost (Figures 3D and 3E) with the SEC11^{L128R} mutation both in vitro and in vivo (Figures 6). The effect of this latter mutation was stronger than that of the SEC11^{P368A} substitution, which was predicted to disrupt SM binding via its major cleft to the closed Qa-SNARE (Misura et al., 2000; Hu et al., 2011), and it was sufficient to prevent secretory rescue by the SM protein in vivo (Figure 7). We can rule out a misfolding of the SEC11^{L128R} since the mutant was nonetheless able to bind with and stabilize the heterotrimeric SNARE complex (Figure 5). Again, the observations were unexpected, but they are in accordance with the novel interaction of SEC11 with the N terminus of the plant Qa-SNAREs. The SEC11^{L103R}, SEC11^{L112R}, and SEC11^{L128R} mutations align with a minor, hydrophobic cleft on the outer surface of mammalian and yeast SM homologs that forms the binding site for the Qa-SNARE N terminus; interactions with this site are thought to initiate the Qa-SNARE in its switch to the open form (Dulubova et al., 1999; Bryant and James, 2001; Bracher and Weissenhorn, 2002; Carpp et al., 2006), but it has not been known to play a major role in binding to the closed Qa-SNARE. However, the loss of binding can be understood if the Qa-SNARE N terminus is essential to stabilize SEC11 interaction with the closed Qa-SNARE through its major cleft of the SM protein. Thus, we suggest that, unlike the mammalian and yeast

cell models, SEC11 association through the SYP121 N terminus is enhanced in the open form of the Qa-SNARE and helps to stabilize its binding to the closed form of SYP121.

A Role for SEC11 Competition in Regulating SYP121-Mediated Vesicle Traffic?

One of the most striking of our observations was that SEC11 appeared to compete for SYP121 binding with its cognate SNAREs SNAP33 and VAMP721 when stabilized through association with the SYP121 N terminus. This competition for SYP121 binding is in accordance with the idea that the SM protein stabilizes the closed form of SYP121. In effect, those molecules bound with SEC11 may be thought to be sequestered and removed from the pool of SYP121 available for assembly in a SNARE complex. The interpretation is consistent also with the findings that the order of additions was important for both SEC11 and SNAP33 binding (Figures 4D to 4F) and that competition was lost with the open form of SYP121 (Figures 4G to 4I). In the latter case, SEC11 binding was unaffected by SNAP33 and VAMP721 additions, but binding of the cognate SNARE was increased significantly when SEC11 was present. Within the limitations of these assays (Rizo et al., 2012), then, the simple interpretation is that SEC11 competition occurs prior to assembly of the SNARE complex, and once the complex is formed, SEC11 binding helps stabilize the complex.

How does interaction between SEC11 and the SYP121 N terminus contribute to these events? One final set of experiments with the SEC11^{L128R} mutant sheds some light here. We found this mutation virtually eliminated SYP121 binding in the absence of its cognate SNAREs (Figure 3), but binding was recovered when SEC11^{L128R} was incubated together with SNAP33 and VAMP721, both with the wild-type and open forms of SYP121 (Figures 5A and 5C); furthermore, its binding, and that of SNAP33 (Figures 5B and 5D), showed no dependence on the order of additions. Clearly, SEC11^{L128R} binding was restricted to the SNARE complex, and the observations lead to a set of simple conclusions: (1) SEC11 binding to the complex occurs independent of its association with the SYP121 N terminus, and as a corollary, (2) its association with the SYP121 N terminus plays a primary role in stabilizing the closed form of the Qa-SNARE. One caveat to these conclusions is their reliance on in vitro analysis and the associated challenge of quantification (Rizo et al., 2012); nonetheless, it remains difficult to accommodate the biochemical data, the consequences of single-site mutations, and supporting in vivo analyses (Figures 1, 2, 6, and 7) in another qualitative context, without additional and ad hoc assumptions. The schematic in Figure 8 summarizes these observations in a comprehensive form. Like the mammalian and yeast models (Jahn and Scheller, 2006; Shen et al., 2007), our data support a mechanism in which SNARE complex assembly is predicated on conversion of the Qa-SNARE to an open, fusion-competent form and, once assembled, the complex is stabilized by binding of the SM protein. Unlike the nonplant models (Tareste et al., 2008; Rathore et al., 2010), we must account for the apparent stabilization of SEC11 binding by the SYP121 N terminus and open conformation (Figures 2 and 3). Thus, we suggest that transition from the SEC11-bound, closed SYP121 to its open, fusion-competent form is not initiated by association with the SYP121 N terminus per se. Instead, we propose that this step of the process requires an additional factor that alters or disrupts SEC11 association with the SYP121 N terminus in order to convert an open-occluded form of the Qa-SNARE, bound with SEC11, to an open-fusion-ready form with SEC11 unbound. In effect, we postulate that SEC11 binding processes through a handshaking sequence with an as yet unknown factor, exchanging between SEC11 bound to the Qa-SNARE in the closed conformation and its stabilization with an open-occluded form, and binding to an open form of the Qa-SNARE assembled within the SNARE complex. Therefore, it is of interest that recent studies have identified members of the Kv-like K^+ channel family in *Arabidopsis* as binding partners of SYP121 (Honsbein et al., 2009, 2011). Significantly, these channels bind to the N terminus of SYP121, and their binding is also sensitive to mutation of the Phe residue at position nine (Grefen et al., 2010a; Honsbein et al., 2011). Thus, we can picture a role for K^+ channel binding in releasing the association of SEC11 with the SYP121 N terminus, the effect in turn being to destabilize SEC11 binding to the open-occluded intermediate of SYP121 and to initiate SNARE complex assembly.

In conclusion, we find that the SM protein SEC11 binds with the Qa-SNARE SYP121 in *Arabidopsis* and is sufficient to rescue secretory traffic block by the dominant-negative SYP121$^{\Delta C}$ protein. Binding occurs differentially between two major modes, one that appears to be associated with an inactive, closed form of SYP121 and the second that is dependent on assembly of the SNARE complex. Consistent with previous work (Park et al., 2012), SEC11 binding to SYP121 is enhanced in a SYP121 mutant thought to favor its open conformation. However, binding to this mutant does not appear to translate to enhanced binding in the SNARE complex. Instead, SEC11 competes for SYP121 binding with its cognate SNAREs. Both this competition and enhanced binding to the open SYP121 are lost when SEC11 interaction with the SYP121 N terminus is suppressed by single-site mutations in the SYP121 N terminus or on the external surface of SEC11. The same SEC11 mutation also precludes secretory traffic rescue in vivo. We propose a model for SYP121-driven fusion in which its activation requires one or more additional factors to relax SEC11 binding to the closed (inactive) form of SYP121 by releasing SEC11 association with the SYP121 N terminus.

METHODS

Plasmids and Recombinant Proteins

Escherichia coli expression clones with appropriate tags were prepared using classical and Gateway cloning. Vector pGEX-4T1 (GE Healthcare) was modified using the Gateway conversion kit (Life Technologies) to include Gateway cloning sites used for expressing N-terminal GST-tagged SNAP33, VAMP721, the SEC11 wild type, and mutants. SYP121$^{\Delta C}$ wild type and mutants were PCR amplified adding 5′ *Nde*I and 3′ *Sal*I sites; these genes were introduced into the pETDuet vector (Carpp et al., 2006) via *Nde*I-*Xho*I. Supplemental Table 1 online lists all the constructs used in this study and their general cloning strategy. Mutations in SYP121 and SEC11 were introduced by site-directed mutagenesis. Primers were designed as described previously introducing silent mutations to distinguish mutants on the DNA level (Horak et al., 2008; Grefen et al., 2010a).

Protein–protein interaction analysis was performed after cloning in the tricistronic vector pBiFCt-2in1-NC for rBiFC as described previously (Grefen and Blatt, 2012). All recombination reactions were achieved with entry clones containing the relevant coding sequences for SEC11, iLOV, SYP121$^{\Delta C}$, and mutants. For rBiFC analysis, SEC11 was tagged N-terminally with nYFP and the SNARE variants C-terminally with cYFP.

For quantitative secretion analysis, an analogous, tetracistronic vector was constructed with Gateway-compatible sites. An expression cassette containing 35S promoter, Omega Enhancer, and secYFP was derived from the pVKH-N-secYFP template (Geelen et al., 2002), flanked by *Afe*I and *Sma*I on the 5′-end and *Mfe*I on the 3′-end, and was generated by PCR and ligated into pBiFC-BB (Grefen and Blatt, 2012) via *Afe*I and *Mfe*I to replace the RFP expression cassette in pBiFC-BB. The expression cassette containing 35S, Omega Enhancer, and GFP-HDEL was PCR amplified from pVKH-GFP-HDEL (Batoko et al., 2000) and ligated into pBiFC-BB-secYFP via the *Sma*I site, resulting in the vector pTecG. The two 2in1 expression cassettes containing 35S promoter, Omega Enhancer, Gateway cassette (either attR3-lacZ-attR2 or attR1-ChloramphenicolR, ccdB-attR4), and a C-terminal tag (either 3xHA or myc) were gene synthesized and sequentially ligated via blunt end cloning (*Afe*I and *Sna*BI) into pTecG to create pTecG-2in1-CC. Secretion analysis was performed with SEC11 untagged as a result of inserting of a stop, and SYP121$^{\Delta C}$ and its mutants were C-terminally myc tagged.

Plant Growth and Extraction

Arabidopsis thaliana syp121-1 mutant plants were complemented with each of the SYP121 mutants, SYP121^{F9A} and SYP121^{S10A} (Grefen et al., 2010a), driven by the mild, constitutive pUB10 promoter (Grefen et al., 2010b). Six-week-old plants were transformed by floral dipping using the method of Clough and Bent (1998). Seed of the wild-type (Columbia-0) parent line, the *syp121-1* mutant, and the T3 generation complemented lines were grown on soil under a 10:14 h light:dark cycle with 150 μmol m^{-2} s^{-1} PAR at 18:23°C. Plants were harvested 14 d after germination, washed, flash-frozen, and ground in liquid N_2. Equal weights of ground tissue were suspended by sonication in equal volumes of homogenization buffer containing 500 mM Suc, 10% glycerol, 20 mM EDTA, 20 mM EGTA, Roche protease inhibitor, 10 mM ascorbic acid, 5 mM DTT, and 50 mM Tris-HCl, pH 7.4, before centrifuging at 13,000*g* for 30 min at 4°C to remove cellular debris. The resulting extracts were diluted 1:1 in 50 mM Tris-HCl, pH 7.4, and 150 mM NaCl for pull-down experiments.

Protein Binding

Vector plasmids were transformed into *E. coli* BL21 DE3 cells (Life Technologies). Expression of the tagged proteins was induced using 1 mM isopropyl β-D-1-thiogalactopyranoside, and cells were harvested after 4 h, lysed, and the supernatant loaded on affinity resin columns for purification according to the manufacturers' instructions. Proteins tagged with GST and 2PA were purified by affinity chromatography with glutathione-coupled Sepharose 4B and IgG Sepharose resins, respectively (GE Healthcare). Following elution, the proteins were dialyzed with two changes of buffer containing 150 mM NaCl, 2.5% glycerol, and 100 mM Tris, pH 8.0, and were verified by immunoblot analysis (see Supplemental Figure 1 online).

Bait proteins were immobilized at a rate of 1 μg/10 μL of affinity resin. Controls included GST or 2PA, and, unless noted, their bound values were subtracted as background in the data reported. Equimolar quantities of the prey proteins were added to the pull-down suspensions in the presence of 100 mM Tris, pH 8.0, and were incubated with gentle mixing for 4 h at 4°C. For complex assays with sequential additions, 4-h incubations were used for each step. Thereafter, each resin was washed with 10× volumes of buffer containing 150 mM NaCl, 1 mM DTT, 0.05% Tween 20, and 100 mM Tris-HCl, pH 8.0, at 4°C, and proteins were eluted by boiling at 95°C for 10 min in Laemmli buffer containing 2.5% 2-mercaptoethanol (Laemmli, 1970). Eluted proteins were separated by SDS-PAGE on 10% acrylamide and proteins analyzed by Coomassie staining and immunoblot with anti-GST antibodies (GE Healthcare). For pull-down assays with *Arabidopsis* fractions, wild-type and mutant SYP121 were detected using polyclonal anti-SYP121 antibodies (Tyrrell et al., 2007) using ECL Advance (GE Healthcare), and the Ponceau-stained ribulose-1,5-bis-phosphate carboxylase/oxygenase bands were used as loading standards. All blots and stained gels were scanned at 1200-dpi resolution, and band intensities were quantified using ImageJ v. 4.3j (rsbweb.nih.gov/ij/) to obtain bound:bait ratios for comparisons within any one experiment and were normalized to standard controls between experiments using the same combinations of proteins.

Confocal Microscopy

Images were collected using a Zeiss LSM510-META confocal microscope with ×20/0.75–numerical aperture and ×40/1.3–numerical aperture objectives. Excitation intensities, filter settings, and photomultiplier gains were standardized (Tyrrell et al., 2007; Grefen et al., 2010b). For rBiFC analysis, YFP and RFP were excited by the 514-nm line of an argon laser and the 543-nm line of a HeNe laser, respectively. YFP fluorescence was collected after passage through a 515-nm dichroic mirror and 535- to 590-nm band-pass filter. RFP fluorescence was collected after passage through a 560-nm dichroic mirror and 560- to 615-nm band-pass filter. For trafficking studies, GFP and YFP were excited by the 458- and 514-nm lines, respectively, of an argon laser, and fluorescence was collected after separation by a 545-nm dichroic mirror. GFP and YFP fluorescence signals were collected after passage through 475- to 525-nm and 535- to 590-nm band-pass filters, respectively. Interference from chlorophyll fluorescence was monitored after passage through a 635-nm dichroic mirror using the META collector set to collect across 638 to 700 nm.

Statistical Analysis

All data are reported as means ± SE of *n* independent measurements. Significance was determined using analysis of variance with significance thresholds as indicated.

Accession Numbers

Sequence data from this article can be found in the Arabidopsis Genome Initiative or GenBank/EMBL databases under the following accession numbers: SYP121 (At3g11820), SEC11 (At1g12360), SYP21 (At5g16830), VAMP721 (At1G04750), and SNAP33 (At5G01010).

Supplemental Data

The following materials are available in the online version of this article.

Supplemental Figure 1. Purification of *Arabidopsis* SNARE and Related Proteins Following Expression in *E. coli*.

Supplemental Figure 2. Coomassie-Stained Gel Showing Proteins Recovered in Pull-Down Assays with SYP121$^{\Delta C}$ Together with GST, GST-SEC11, and GST-iLOV as Baits.

Supplemental Table 1. Primer Sequences Used for Cloning SEC11, VAMP721, and SNAP33 and for Site-Directed Mutagenesis of SEC11.

ACKNOWLEDGMENTS

We thank John Christie for the pGEX-iLOV construct. This work was funded by Grants BB/H009817/1 and BB/H024867/1 from the Biotechnology and Biological Sciences Research Council. R.B. was supported by a Summer

Undergraduate Research Fellow award from the American Society of Plant Biologists.

AUTHOR CONTRIBUTIONS

R.K. established the purification protocols and carried out the pull-down assays and BiFC studies with support from R.B., T.K., and M.R.B. C.G. developed the vector systems and the tetracistronic vector for secretion analysis. R.K. and C.G. carried out the cloning. M.W. advised on the article and developed Figure 8. M.R.B., N.J.B., and R.K. wrote the article. A.H. initiated work to purify the protein domains with guidance from D.K.

Received December 14, 2012; revised February 27, 2013; accepted March 16, 2013; published April 9, 2013.

REFERENCES

Aran, V., Brandie, F.M., Boyd, A.R., Kantidakis, T., Rideout, E.J., Kelly, S.M., Gould, G.W., and Bryant, N.J. (2009). Characterization of two distinct binding modes between syntaxin 4 and Munc18c. Biochem. J. **419:** 655–660.

Assaad, F.F., Huet, Y., Mayer, U., and Jürgens, G. (2001). The cytokinesis gene KEULE encodes a Sec1 protein that binds the syntaxin KNOLLE. J. Cell Biol. **152:** 531–543.

Bassham, D.C., and Blatt, M.R. (2008). SNAREs: Cogs and coordinators in signaling and development. Plant Physiol. **147:** 1504–1515.

Bassham, D.C., Sanderfoot, A.A., Kovaleva, V., Zheng, H.Y., and Raikhel, N.V. (2000). AtVPS45 complex formation at the trans-Golgi network. Mol. Biol. Cell **11:** 2251–2265.

Batoko, H., Zheng, H.Q., Hawes, C., and Moore, I. (2000). A rab1 GTPase is required for transport between the endoplasmic reticulum and Golgi apparatus and for normal Golgi movement in plants. Plant Cell **12:** 2201–2218.

Blatt, M.R., Leyman, B., and Geelen, D. (1999). Molecular events of vesicle trafficking and control by SNARE proteins in plants. New Phytol. **144:** 389–418.

Blatt, M.R., and Thiel, G. (2003). SNARE components and mechanisms of exocytosis in plants. In The Golgi Apparatus and the Plant Secretory Pathway, D.G. Robinson, ed (Oxford, UK: Blackwell Publishing, CRC Press), pp. 208–237.

Bock, J.B., Matern, H.T., Peden, A.A., and Scheller, R.H. (2001). A genomic perspective on membrane compartment organization. Nature **409:** 839–841.

Boevink, P., Oparka, K., Santa Cruz, S., Martin, B., Betteridge, A., and Hawes, C. (1998). Stacks on tracks: The plant Golgi apparatus traffics on an actin/ER network. Plant J. **15:** 441–447.

Bracher, A., Perrakis, A., Dresbach, T., Betz, H., and Weissenhorn, W. (2000). The X-ray crystal structure of neuronal Sec1 from squid sheds new light on the role of this protein in exocytosis. Structure **8:** 685–694.

Bracher, A., and Weissenhorn, W. (2002). Structural basis for the Golgi membrane recruitment of Sly1p by Sed5p. EMBO J. **21:** 6114–6124.

Bryant, N.J., and James, D.E. (2001). Vps45p stabilizes the syntaxin homologue Tlg2p and positively regulates SNARE complex formation. EMBO J. **20:** 3380–3388.

Burgoyne, R.D., and Morgan, A. (2007). Membrane trafficking: Three steps to fusion. Curr. Biol. **17:** R255–R258.

Calakos, N., Bennett, M.K., Peterson, K.E., and Scheller, R.H. (1994). Protein-protein interactions contributing to the specificity of intracellular vesicular trafficking. Science **263:** 1146–1149.

Carpp, L.N., Ciufo, L.F., Shanks, S.G., Boyd, A., and Bryant, N.J. (2006). The Sec1p/Munc18 protein Vps45p binds its cognate SNARE proteins via two distinct modes. J. Cell Biol. **173:** 927–936.

Chapman, S., Faulkner, C., Kaiserli, E., Garcia-Mata, C., Savenkov, E.I., Roberts, A.G., Oparka, K.J., and Christie, J.M. (2008). The photoreversible fluorescent protein iLOV outperforms GFP as a reporter of plant virus infection. Proc. Natl. Acad. Sci. USA **105:** 20038–20043.

Clough, S.J., and Bent, A.F. (1998). Floral dip: A simplified method for Agrobacterium-mediated transformation of *Arabidopsis thaliana*. Plant J. **16:** 735–743.

Collins, N.C., Thordal-Christensen, H., Lipka, V., Bau, S., Kombrink, E., Qiu, J.L., Hückelhoven, R., Stein, M., Freialdenhoven, A., Somerville, S.C., and Schulze-Lefert, P. (2003). SNARE-protein-mediated disease resistance at the plant cell wall. Nature **425:** 973–977.

Dulubova, I., Khvotchev, M., Liu, S.Q., Huryeva, I., Südhof, T.C., and Rizo, J. (2007). Munc18-1 binds directly to the neuronal SNARE complex. Proc. Natl. Acad. Sci. USA **104:** 2697–2702.

Dulubova, I., Sugita, S., Hill, S., Hosaka, M., Fernandez, I., Südhof, T.C., and Rizo, J. (1999). A conformational switch in syntaxin during exocytosis: Role of munc18. EMBO J. **18:** 4372–4382.

Dulubova, I., Yamaguchi, T., Gao, Y., Min, S.W., Huryeva, I., Südhof, T.C., and Rizo, J. (2002). How Tlg2p/syntaxin 16 'snares' Vps45. EMBO J. **21:** 3620–3631.

Eisenach, C., Chen, Z.H., Grefen, C., and Blatt, M.R. (2012). The trafficking protein SYP121 of *Arabidopsis* connects programmed stomatal closure and K^+ channel activity with vegetative growth. Plant J. **69:** 241–251.

Fasshauer, D., Sutton, R.B., Brunger, A.T., and Jahn, R. (1998). Conserved structural features of the synaptic fusion complex: SNARE proteins reclassified as Q- and R-SNAREs. Proc. Natl. Acad. Sci. USA **95:** 15781–15786.

Geelen, D., Leyman, B., Batoko, H., Di Sansebastiano, G.P., Moore, I., and Blatt, M.R. (2002). The abscisic acid-related SNARE homolog NtSyr1 contributes to secretion and growth: Evidence from competition with its cytosolic domain. Plant Cell **14:** 387–406. Erratum. Plant Cell **14:** 963.

Grefen, C., and Blatt, M.R. (2008). SNAREs—Molecular governors in signalling and development. Curr. Opin. Plant Biol. **11:** 600–609.

Grefen, C., and Blatt, M.R. (2012). A 2in1 cloning system enables ratiometric bimolecular fluorescence complementation (rBiFC). Biotechniques **2012:** 311–314.

Grefen, C., Chen, Z.H., Honsbein, A., Donald, N., Hills, A., and Blatt, M.R. (2010a). A novel motif essential for SNARE interaction with the $K(^+)$ channel KC1 and channel gating in *Arabidopsis*. Plant Cell **22:** 3076–3092.

Grefen, C., Donald, N., Hashimoto, K., Kudla, J., Schumacher, K., and Blatt, M.R. (2010b). A ubiquitin-10 promoter-based vector set for fluorescent protein tagging facilitates temporal stability and native protein distribution in transient and stable expression studies. Plant J. **64:** 355–365.

Halachmi, N., and Lev, Z. (1996). The Sec1 family: A novel family of proteins involved in synaptic transmission and general secretion. J. Neurochem. **66:** 889–897.

Honsbein, A., Blatt, M.R., and Grefen, C. (2011). A molecular framework for coupling cellular volume and osmotic solute transport control. J. Exp. Bot. **62:** 2363–2370.

Honsbein, A., Sokolovski, S., Grefen, C., Campanoni, P., Pratelli, R., Paneque, M., Chen, Z.H., Johansson, I., and Blatt, M.R. (2009). A tripartite SNARE-K^+ channel complex mediates in channel-dependent K^+ nutrition in *Arabidopsis*. Plant Cell **21:** 2859–2877.

Horak, J., Grefen, C., Berendzen, K.W., Hahn, A., Stierhof, Y.D., Stadelhofer, B., Stahl, M., Koncz, C., and Harter, K. (2008). The *Arabidopsis thaliana* response regulator ARR22 is a putative AHP phospho-histidine phosphatase expressed in the chalaza of developing seeds. BMC Plant Biol. **8:** 77.

Hu, K., Carroll, J., Fedorovich, S., Rickman, C., Sukhodub, A., and Davletov, B. (2002). Vesicular restriction of synaptobrevin suggests a role for calcium in membrane fusion. Nature **415:** 646–650.

Hu, S.H., Christie, M.P., Saez, N.J., Latham, C.F., Jarrott, R., Lua, L.H.L., Collins, B.M., and Martin, J.L. (2011). Possible roles for Munc18-1 domain 3a and Syntaxin1 N-peptide and C-terminal anchor in SNARE complex formation. Proc. Natl. Acad. Sci. USA **108:** 1040–1045.

Hughson, F.M. (2013). Neuroscience. Chaperones that SNARE neurotransmitter release. Science **339:** 406–407.

Jahn, R., and Scheller, R.H. (2006). SNAREs—Engines for membrane fusion. Nat. Rev. Mol. Cell Biol. **7:** 631–643.

Kargul, J., Gansel, X., Tyrrell, M., Sticher, L., and Blatt, M.R. (2001). Protein-binding partners of the tobacco syntaxin NtSyr1. FEBS Lett. **508:** 253–258.

Khvotchev, M., Dulubova, I., Sun, J., Dai, H., Rizo, J., and Südhof, T.C. (2007). Dual modes of Munc18-1/SNARE interactions are coupled by functionally critical binding to syntaxin-1 N terminus. J. Neurosci. **27:** 12147–12155.

Kwon, C., et al. (2008). Co-option of a default secretory pathway for plant immune responses. Nature **451:** 835–840.

Laemmli, U.K. (1970). Cleavage of structural proteins during the assembly of the head of bacteriophage T4. Nature **227:** 680–685.

Leyman, B., Geelen, D., Quintero, F.J., and Blatt, M.R. (1999). A tobacco syntaxin with a role in hormonal control of guard cell ion channels. Science **283:** 537–540.

Lipka, V., Kwon, C., and Panstruga, R. (2007). SNARE-ware: The role of SNARE-domain proteins in plant biology. Annu. Rev. Cell Dev. Biol. **23:** 147–174.

Ma, C., Su, L., Seven, A.B., Xu, Y., and Rizo, J. (2013). Reconstitution of the vital functions of Munc18 and Munc13 in neurotransmitter release. Science **339:** 421–425.

Margittai, M., Fasshauer, D., Jahn, R., and Langen, R. (2003). The Habc domain and the SNARE core complex are connected by a highly flexible linker. Biochemistry **42:** 4009–4014.

Misura, K.M.S., Scheller, R.H., and Weis, W.I. (2000). Three-dimensional structure of the neuronal-Sec1-syntaxin 1a complex. Nature **404:** 355–362.

Park, M., Touihri, S., Müller, I., Mayer, U., and Jürgens, G. (2012). Sec1/Munc18 protein stabilizes fusion-competent syntaxin for membrane fusion in Arabidosis cytokinesis. Dev. Cell **22:** 989–1000.

Peng, R.W., and Gallwitz, D. (2004). Multiple SNARE interactions of an SM protein: Sed5p/Sly1p binding is dispensable for transport. EMBO J. **23:** 3939–3949.

Pratelli, R., Sutter, J.-U., and Blatt, M.R. (2004). A new catch in the SNARE. Trends Plant Sci. **9:** 187–195.

Rathore, S.S., Bend, E.G., Yu, H.J., Hammarlund, M., Jorgensen, E.M., and Shen, J.S. (2010). Syntaxin N-terminal peptide motif is an initiation factor for the assembly of the SNARE-Sec1/Munc18 membrane fusion complex. Proc. Natl. Acad. Sci. USA **107:** 22399–22406.

Rizo, J., Rosen, M.K., and Gardner, K.H. (2012). Enlightening molecular mechanisms through study of protein interactions. J. Mol. Cell Biol. **4:** 270–283.

Rojo, E., Zouhar, J., Kovaleva, V., Hong, S., and Raikhel, N.V. (2003). The AtC-VPS protein complex is localized to the tonoplast and the prevacuolar compartment in Arabidosis. Mol. Biol. Cell **14:** 361–369.

Sanderfoot, A.A., Assaad, F.F., and Raikhel, N.V. (2000). The *Arabidopsis* genome. An abundance of soluble N-ethylmaleimide-sensitive factor adaptor protein receptors. Plant Physiol. **124:** 1558–1569.

Shen, J., Rathore, S.S., Khandan, L., and Rothman, J.E. (2010). SNARE bundle and syntaxin N-peptide constitute a minimal complement for Munc18-1 activation of membrane fusion. J. Cell Biol. **190:** 55–63.

Shen, J.S., Tareste, D.C., Paumet, F., Rothman, J.E., and Melia, T.J. (2007). Selective activation of cognate SNAREpins by Sec1/Munc18 proteins. Cell **128:** 183–195.

Südhof, T.C., and Rothman, J.E. (2009). Membrane fusion: Grappling with SNARE and SM proteins. Science **323:** 474–477.

Sutter, J.U., Campanoni, P., Blatt, M.R., and Paneque, M. (2006a). Setting SNAREs in a different wood. Traffic **7:** 627–638.

Sutter, J.U., Campanoni, P., Tyrrell, M., and Blatt, M.R. (2006b). Selective mobility and sensitivity to SNAREs is exhibited by the *Arabidopsis* KAT1 K^+ channel at the plasma membrane. Plant Cell **18:** 935–954.

Sutter, J.U., Sieben, C., Hartel, A., Eisenach, C., Thiel, G., and Blatt, M.R. (2007). Abscisic acid triggers the endocytosis of the *Arabidopsis* KAT1 K+ channel and its recycling to the plasma membrane. Curr. Biol. **17:** 1396–1402.

Sutton, R.B., Fasshauer, D., Jahn, R., and Brunger, A.T. (1998). Crystal structure of a SNARE complex involved in synaptic exocytosis at 2.4 A resolution. Nature **395:** 347–353.

Tareste, D., Shen, J., Melia, T.J., and Rothman, J.E. (2008). SNAREpin/Munc18 promotes adhesion and fusion of large vesicles to giant membranes. Proc. Natl. Acad. Sci. USA **105:** 2380–2385.

Tyrrell, M., Campanoni, P., Sutter, J.-U., Pratelli, R., Paneque, M., Sokolovski, S., and Blatt, M.R. (2007). Selective targeting of plasma membrane and tonoplast traffic by inhibitory (dominant-negative) SNARE fragments. Plant J. **51:** 1099–1115.

Waizenegger, I., Lukowitz, W., Assaad, F., Schwarz, H., Jürgens, G., and Mayer, U. (2000). The *Arabidopsis KNOLLE* and *KEULE* genes interact to promote vesicle fusion during cytokinesis. Curr. Biol. **10:** 1371–1374.

Weber, T., Zemelman, B.V., McNew, J.A., Westermann, B., Gmachl, M., Parlati, F., Söllner, T.H., and Rothman, J.E. (1998). SNAREpins: Minimal machinery for membrane fusion. Cell **92:** 759–772.

Zouhar, J., Rojo, E., and Bassham, D.C. (2009). AtVPS45 is a positive regulator of the SYP41/SYP61/VTI12 SNARE complex involved in trafficking of vacuolar cargo. Plant Physiol. **149:** 1668–1678.